Enhanced Knowledge in Sciences and Technology Vol. 2 No. 2 (2022) 052-059

EKST

Homepage: http://publisher.uthm.edu.my/periodicals/index.php/ekst
e-ISSN : 2773-6385

Effect of Sintering Temperature on Structural and Surface Morphology of Manganite: $Pr_{0.75}Na_{0.25-x}Ag_xMnO_3$

Wilson Teoh Wei Sheng[1], Suhadir Shamsuddin[2]*

[1,2*]Ceramic and Amorphous Group, Faculty of Applied Sciences and Technology, Universiti Tun Hussein Onn Malaysia, 84600 Pagoh, Johor, MALAYSIA

*Corresponding Author Designation

DOI: https://doi.org/10.30880/ekst.2022.02.02.006
Received 02 January 2022; Accepted 02 March 2022; Available online 23 November 2022

Abstract: Monovalent doped $Pr_{0.75}Na_{0.2}Ag_{0.05}MnO_3$ manganite had been investigated to elucidate the effect of sintering temperature on the structural, surface morphology, density as well as porosity of perovskite manganite. While Ag^+ ions has been seen in previous studies to show successful substitution and improvement to structural characteristics, the effect on sintering temperature towards the manganite has not yet been investigated. The manganite samples were prepared with Pr_2O_3, Na_2CO_3, Ag_2O and MnO_2 powders of high purity using solid state reaction method. The structural characterisation was made using X-ray diffraction (XRD) and scanning electron microscope (SEM) equipped with energy dispersion x-ray spectroscopy (EDX) to investigate the surface morphology imaging and elemental composition analysis. The determination of density was done with the application of Archimedes Principle and the calculation of porosity was made using the standard formula. XRD analysis showed all samples were crystallized in an orthorhombic structure of *Pnma* space group with a decrease in unit cell volume as sintering temperature increase. SEM imaging of $Pr_{0.75}Na_{0.2}Ag_{0.05}MnO_3$ compound revealed an improvement on grain size, grain density and boundaries as well as the reduction of porosity with the increase in sintering temperature. The increase in bulk density and the decrease in porosity as sintering temperature rises were also confirmed through calculation using the lattice parameter of the samples analysed by XRD. The samples were shown to have the same composition without any impurities through EDX analysis. Hence, the correlation between XRD and SEM can be observed with the results from both analyses equipment showing a good agreement.

Keywords: X-ray Diffraction, Scanning Electron Microscope, Energy Dispersive X-Ray Spectroscopy

Corresponding author: suhadir@uthm.edu.my

1. Introduction

Perovskite manganite materials have been a topic of debate for researchers in the recent years due to their intriguing properties. Perovskite manganite can be found in nature where they exhibit insulator behaviour. Although manganites originally exist to have an antiferromagnetic (AFM) ordering, special properties can be seen through doping process where the rendering of the $LaMnO_3$ manganite intro ferromagnetic (FM) and metallic state through substitution process of La^{3+} with a divalent or monovalent cation [1]. The perovskite-type manganite $Ln_{1-x}A_xMnO3$, where Ln represent lanthanum or rare-earth element and A for alkaline metals have been extensively studied in view of the observed colossal magnetoresistance (CMR) of these compounds and the potential applications with the magnetic properties of the compound [2]. Throughout the studies on perovskite manganites, monovalent-doped manganites tend to show special properties on the structural and surface morphology when doping of monovalent metal is introduced. [1,3-4]. Moreover, the study has shown there was a revival of double-exchange (DE) mechanism that led to the weakening of charger-order (CO) state with the reduction of John-Teller effect where further research has been done to understand the effect towards electrical transport [4-5]. Studies have been carried out by varying the amount of dopant towards the parent compounds to investigate their effect and changes towards electrical, magnetic, composition and the crystalline structure [6-8]. However, there is a lack of investigation that reports on the effect of sintering temperature towards perovskite manganites. As samples undergo sintering process to allow the growth of the crystalline, it is undeniable that sintering temperature has a significant role on the formation of crystalline structure as well as its characteristic such as density and porosity [9].

In this study, the $Pr_{0.75}Na_{0.2}Ag_{0.05}MnO_3$ manganite is synthesised to study the effect of sintering temperature towards the structural and surface morphology of the manganite compound. The reason for using Ag as dopant is due to Ag^+ ions has been seen in previous studies to show successful substitution within perovskite manganite and delivers enhancement to the grain boundaries, sizes as well as the compaction [4-5]. Further study on the manganite towards the effect of different sintering temperature enables a better understanding towards the changes in structural properties such as crystalline structure and the composition as well as surface morphology including the grain size, boundaries, density, as well as porosity.

2. Materials and Methods

The Ag-doped $Pr_{0.75}Na_{0.2}Ag_{0.05}MnO_3$ manganite samples were prepared using solid state reaction method. For sample characterisation, X-ray diffraction was used to study the crystalline structure while the surface morphology of samples along with the elemental compositions were investigated using scanning electron microscope equipped with energy dispersive X-ray analysis. Archimedes Principle was applied to determine the density of samples whereas the porosity was obtained through calculation using the standard formula which based on bulk density and theoretical density.

2.1 Chemical and apparatus

The chemicals used for synthesising the samples were Pr_2O_3, Na_2CO_3, Ag_2O and MnO_2 powder of high purity (99.99%). The apparatuses needed in preparation of samples were high sensitivity digital electronic balance EJ-OP-13 Density Determination Kit, agate mortar and the pestle, alumina crucible, Protherm Furnace PLF 130/15 box furnace, and Carver model 3851-0 hydraulic press. The equipment required for the characterisation process were Bruker D8 Advance model powder X-ray diffraction and Coxem EM-30AX Plus model scanning electron microscope.

2.2 Sample Preparation

The synthesis of sample compound $Pr_{0.75}Na_{0.2}Ag_{0.05}MnO_3$ was carried out by applying the solid-state reaction method. A stoichiometric mixture of high purity (>99.99%) Pr_2O_3, Na_2CO_3, Ag_2O and MnO_2 powders were mixed and grinded carefully. The process was followed by calcination for 24 hours at a temperature 1000°C with several intermediate grindings. The powder was then pressed into pellet form with a 13mm diameter and 2-3mm thickness under the pressure of 5 tones. Finally, the pelleted samples were then sintered at 1100°C, 1150°C and 1200°C for 24 hours in air. The structural characterisation of the samples was made using Bruker D8 Advance model powder X-ray diffraction (XRD) with Cu Kα radiation at room temperature. The surface morphology of the samples was studied using Coxem EM-30AX Plus model scanning electron microscope (SEM) at magnification of 5kX. Energy dispersive X-ray spectroscopy (EDX) analysis was also done using SEM to determine the elemental composition of the samples.

2.3 Equations of Bulk and Theoretical Density, Porosity and Lattice Parameter

The bulk density of the samples was obtained by applying Archimedes principle where the buoyant medium used was acetone. The weight of sample in air and propanol was measured using compact precision balance. The bulk density was then calculated using Equation 1 [3-4]

$$\rho_{\text{bulk}} = \frac{w_{\text{air}}}{w_{\text{air}} - w_{\text{acetone}}} \rho_{acetone} \qquad Eq.1$$

where w_{air} is the weight of the sample in air, w_{acetone} is the weight of the sample when immersed in acetone and ρ_{acetone} is the density of the acetone. As for the porosity, it was determined from Equation 2 [3-4]

$$\text{Porosity (\%)} = \left(1 - \frac{\rho_{\text{bulk}}}{\rho_{theoretical}}\right) \times 100\% \qquad Eq.2$$

where ρ_{bulk} is the bulk density of the sample obtained from Equation 1 and the value $\rho_{theoretical}$ is the theoretical density of the sample calculated from XRD measurement using Equation 3 [3-4]

$$\rho_{theoretical} = \frac{n'(\sum A_c + \sum A_A)}{V_c N_A} \qquad Eq.3$$

where *n'* denote the number of formula units/unit cell, ΣAc as the total atomic weights of cations within the formula units, ΣA_A is the total atomic weight of anions within the formula units, Vc is the unit cell volume and N_A represents Avogadro's numbers.

The information on lattice parameter and unit cell volume were evaluated using UnitCellWin programme to validate the crystalline phase of the samples. The crystalline patterns were then determined and labelled with miller indices (h, k, l), which represent the Bragg's plane. The lattice parameters *a*, *b*, and *c* were determined using formula as shown in Equation 4 [4].

$$\frac{1}{{d_{hkl}}^2} = \frac{h^2}{a^2} + \frac{k^2}{b^2} + \frac{l^2}{c^2} \qquad Eq.4$$

3. Results and Discussion

Figure 1 depict the XRD pattern for $Pr_{0.75}Na_{0.2}Ag_{0.05}MnO_3$ manganite samples sintered at 1100°C, 1150°C and 1200°C. Based on the XRD analysis, all samples were indexed and indicated to have an orthorhombic structure with *Pnma* space group. This shows that sintering temperature does not influence the crystalline structure of the sample [10-12]. There were no obvious impurity peaks as well as secondary peaks from the XRD result. Table 1 demonstrates the result of lattice parameter, unit cell volume, bulk density, and porosity for all the samples. Onto the lattice parameter, *a*-lattice and *c*-lattice undergone an increase then decrease trend whereas *b*-lattice experience a decrease then increase as the

sintering temperature increases. Overall, the result shows that the unit cell volume decreases as sintering temperature increases which may be attributed to the Jahn–Teller distortion and the variation in Mn–O–Mn bond angle. This result can be seen from previous study conducted on $La_{0.67}Ba_{0.3}Mn_{0.9}Cr_{0.1}O_3$ manganite [13]. For bulk density, it is observed to be increasing as the sintering temperature increases. The porosity of the sample also shows a decrease with the rising of temperature as grains tend to become more densely packed [10].

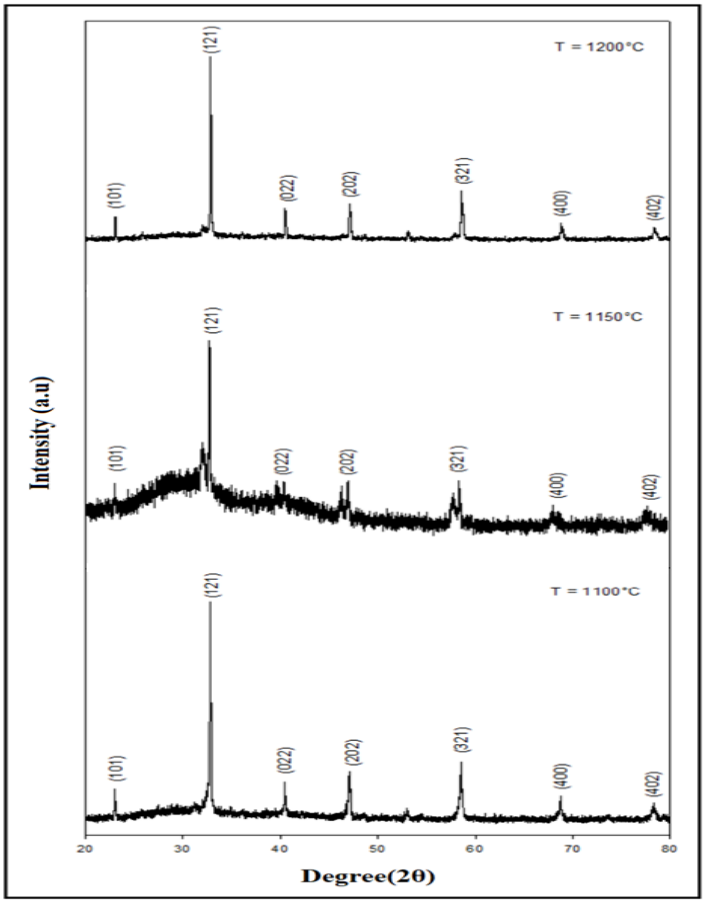

Figure 1: The X-ray Diffraction (XRD) analysis for the sample $Pr_{0.75}Na_{0.2}Ag_{0.05}MnO_3$ sintered at 1100°C, 1150°C and 1200°C

Table 1: Lattice parameters, unit cell volume (V), bulk density (ρ_{bulk}) and porosity of the sample $Pr_{0.75}Na_{0.2}Ag_{0.05}MnO_3$ sintered at 1100°C, 1150°C and 1200°C

Sintering temperature (°C)	Lattice parameter, Å (± 0.001)			V, Å^3 (± 0.1)	ρ_{bulk}, g/cm^3 (± 0.001)	Porosity, % (± 0.01)
	a (Å)	b (Å)	c (Å)			
1100	5.458	7.720	5.454	229.8	4.936	21.89
1150	5.459	7.705	5.458	229.5	5.287	16.43
1200	5.453	7.708	5.451	229.1	6.082	4.030

Figure 2 displays the SEM imaging for all samples with the magnification of 5kX. The SEM images revealed that there is an increase in grain size as the sintering temperature increases where the boundary

samples have become compact and connected and achieve a well-defined grain boundary at sintering temperature of 1200°C. In fact, this can be suggested that sintering temperature can promote the growth of grain size and agglomeration as at higher temperature, the microstructures of grains will be reduced, leaving closely packed grains [11, 13-14]. These characteristics can be observed from the images where there are visible porosities with a decreasing trend as the sintering temperature increases from 1100°C to 1150°C. The agglomeration rate of the grains also increases until the point where there is no obvious visible pore can be seen for sample sintered at 1200°C. This can be due to the growth in grain size as grains tend to form larger particles as temperature raises [11]. By comparing the observation on the number of pores of sample from SEM imaging with the porosity calculated based on the bulk density and lattice parameter from XRD analysis, it be said that the XRD analysis are in line with the SEM imaging where both the results depicted that porosity decreases as sintering temperature rises. This demonstrated a correlation between the two analytical techniques which has shown to have a good agreement.

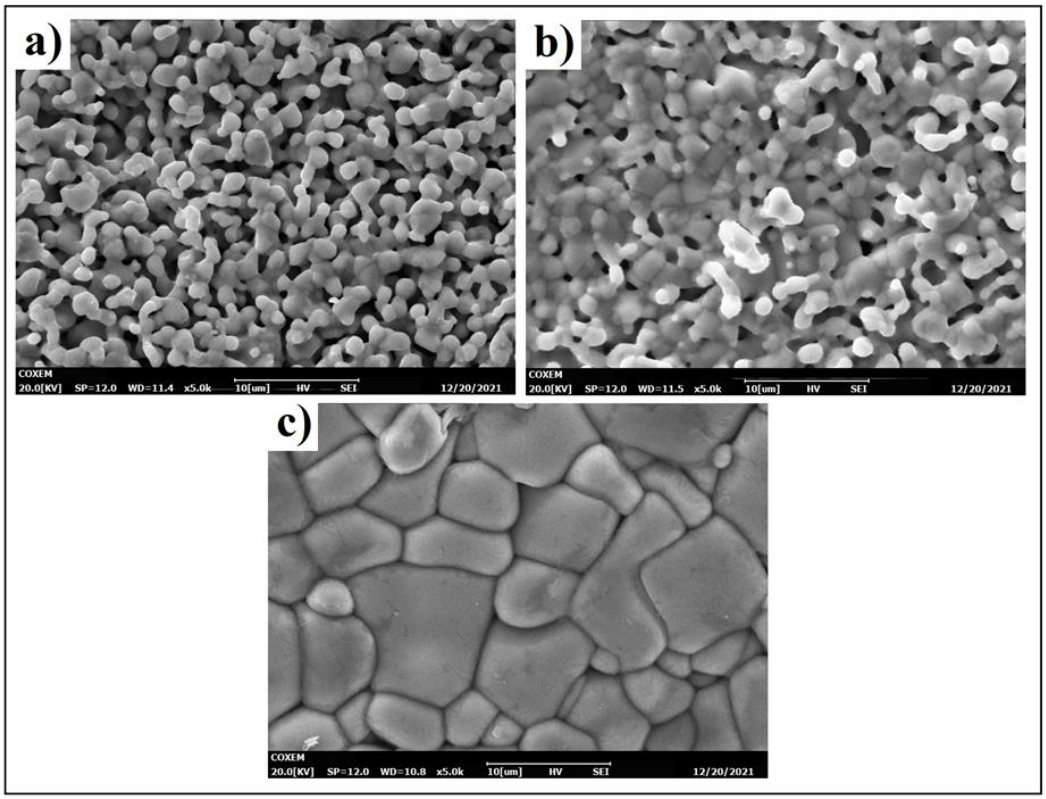

Figure 2: SEM imaging for the sample $Pr_{0.75}Na_{0.2}Ag_{0.05}MnO_3$ sintered at (a)1100°C, (b)1150°C and (c)1200°C with 5kX magnification

Figure 3 illustrates the EDX analysis spectrum for all the samples. According to the spectrum generated, all the constitute elements (Pr, Na, Ag, Mn, O) were confirmed without any impurity which shows that proper synthetization of the sample has been done. On the elemental composition weight percentage, the samples which are sintered at different temperature are according the sociometry proportion calculated during the preparation of the sample. From the result, there is a decrease in atomic weight of Ag dopant as the sintering temperature increases. This may be due to where the increasing of sintering temperature will cause the Ag^+ ions bonded to the perovskite phase to leave the perovskite phase. This conclusion can be made based on previous research which was done on $La_{1-x}Ag_xMnO_3$ manganite samples [15].

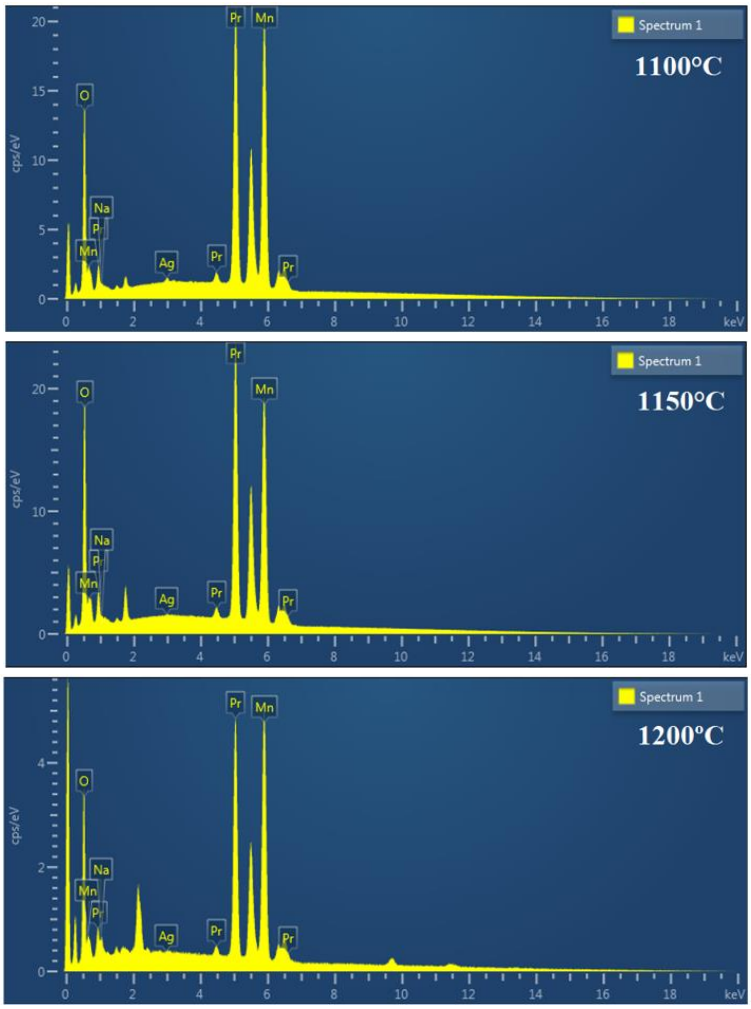

Element	Weight%	Atomic%
Pr	58.37	21.25
Na	0.71	1.57
Ag	0.54	0.26
Mn	23.12	21.59
O	17.26	55.33

Element	Weight%	Atomic%
Pr	58.95	19.91
Na	0.79	1.63
Ag	0.11	0.05
Mn	19.46	16.86
O	20.69	61.55

Element	Weight%	Atomic%
Pr	55.61	19.43
Na	2.37	5.07
Ag	0.08	0.04
Mn	24.58	22.03
O	17.37	53.44

Figure 3: EDX spectrum for the sample $Pr_{0.75}Na_{0.2}Ag_{0.05}MnO_3$ with sintering temperature of 1100°C, 1150°C and 1200°C

4. Conclusion

In general, the increment of sintering temperature improves the crystalline structure as well as the surface morphology of the $Pr_{0.75}Na_{0.2}Ag_{0.05}MnO_3$ manganite compound. While the difference in sintering temperature does not affect the crystalline structure, it has also been observed to have influence towards the density, grain size as well as porosity of the samples. The elemental composition of the sample shows that the sample does not being affected by the varying sintering temperature. Throughout this study, the effect of sintering temperature has provided some clarification on the structural and surface changes towards the sample manganite compound. Further research and characterisation such as on magnetic properties, electrical properties and ultrasonic anomaly characterisation are recommended to understand more on the influenced of sintering temperature towards the manganite compound.

Acknowledgement

This research was supported by TIER 1 Vot H967 Research Grant from Universiti Tun Hussein Onn Malaysia. Thanks to Ceramic and Amorphous Group, Faculty of Applied Sciences and Technology, Pagoh Higher Education Hub, Universiti Tun Hussein Onn Malaysia, 84600 Panchor, Johor for the facilities provided.

References

[1] S. Kansara, D. Dhruv, B. Kataria, C. Thaker, S. Rayaprol, C. Prajapat, M. Singh, P. Solanki, D. Kuberkar, N. Shah, "Structural, transport and magnetic properties of monovalent doped $La_{1-x}Na_xMnO_3$ manganites", *Ceramics International*, vol. 41, no. 5, pp. 7162-7173, 2015. Available: 10.1016/j.ceramint.2015.02.037.

[2] E. Dagotto, T. Hotta and A. Moreo, "Colossal magnetoresistant materials: the key role of phase separation", *Physics Reports*, vol. 344, no. 1-3, pp. 1-153, 2001. Available: 10.1016/s0370-1573(00)00121-6.

[3] S. Shamsuddin, A. Ibrahim and A. Yahya, "Effects of Cr substitution and oxygen reduction on elastic anomaly and ultrasonic velocity in charge-ordered $Nd_{0.5}Ca_{0.5}Mn_{1-x}Cr_xO_{3-\delta}$ ceramics", *Ceramics International*, vol. 39, pp. S185-S188, 2013. Available: 10.1016/j.ceramint.2012.10.059.

[4] N. Khairulzaman, N. Ibrahim and S. Shamsuddin, "Impact of Ag-Doped on the Ferromagnetic-Metallic Transition in $Pr_{0.75}Na_{0.25}MnO_3$ Manganites", *International Journal of Engineering & Technology*, vol. 7, no. 430, pp. 68, 2018. Available: 10.14419/ijet.v7i4.30.22011.

[5] N. Khairulzaman, N. Ibrahim and S. Shamsuddin, "Effect of Ag-doped on Electrical Transport Properties in $Pr_{0.75}Na_{0.25}MnO_3$ Manganites", *Jour of adv research in dynamical & control systems*, vol. 12, special issue-02, pp. 759-765, 2020.

[6] W. Xia, Z. Pei, K. Leng and X. Zhu, "Research Progress in Rare Earth-Doped Perovskite Manganite Oxide Nanostructures", *Nanoscale Research Letters*, vol. 15, no. 1, 2020. Available: 10.1186/s11671-019-3243-0.

[7] S. Razali, N. Ibrahim, S. Shamsuddin and M. Noh, "Observation of Charge Ordering Signal in Monovalent Doped $Nd_{0.75}Na_{0.25-x}K_xMnO_3$ ($0 \leq x \leq 0.10$) Manganites", *International Journal of Engineering & Technology*, vol. 7, no. 430, p. 85, 2018. Available: 10.14419/ijet.v7i4.30.22021.

[8] M. Xiang, Y. Zhang, Y. Zhang, C. Wang, W. Liu and Y. Yu, "Effects of grain size and porosity on strength of $Li2TiO_3$ tritium breeding pebbles and its grain growth behavior", *Journal of Nuclear Materials*, vol. 482, pp. 163-169, 2016. Available: 10.1016/j.jnucmat.2016.10.027.

[9] R. Frano, D. Aquaro, L. Scaletti and N. Olivi, "Characterization of the thermal conductivity for ceramic pebble beds", *Journal of Physics: Conference Series*, vol. 655, p. 012057, 2015. Available: 10.1088/1742-6596/655/1/012057.

[10] F. Jin, H. Zhang, X. Chen, X. Liu and Q. Chen, "Improvement in electronic and magnetic transport of of $La_{0.67}Ca_{0.33}MnO_3$ manganites by optimizing sintering temperature", *Journal of Sol-Gel Science and Technology*, vol. 81, no. 1, pp. 177-184, 2016. Available: 10.1007/s10971-016-4186-x.

[11] W. Mabrouki, A. Krichene, N. Chniba Boudjada and W. Boujelben, "Sintering temperature effect on the magnetic properties of $Pr_{0.67}Sr_{0.33}MnO_3$ manganite", *Applied Physics A*, vol. 126, no. 3, 2020. Available: 10.1007/s00339-020-3364-4.

[12] M. Bhat, A. Modi and N. Gaur, "The effect of sintering temperature on the magneto-transport properties of $Pr_{0.67}Sr_{0.33-x}Ag_xMnO_3$ ($0 \leq x \leq 0.1$) manganites", *Journal of Materials Science: Materials in Electronics*, vol. 26, no. 9, pp. 6444-6449, 2015. Available: 10.1007/s10854-015-3235-5.

[13] M. Oumezzine, O. Peña, T. Guizouarn, R. Lebullenger and M. Oumezzine, "Impact of the sintering temperature on the structural, magnetic and electrical transport properties of doped $La_{0.67}Ba_{0.3}Mn_{0.9}Cr_{0.1}O_3$ manganite", *Journal of Magnetism and Magnetic Materials*, vol. 324, no. 18, pp. 2821-2828, 2012. Available: 10.1016/j.jmmm.2012.04.017.

[14] Y. Liu, T. Sun, G. Dong, S. Zhang, K. Chu, X. Pu, H. Li, X. Liu, "Dependence on sintering temperature of structure, optical and magnetic properties $La_{0.625}Ca_{0.315}Sr_{0.06}MnO_3$ perovskite nanoparticles", *Ceramics International*, vol. 45, no. 14, pp. 17467-17475, 2019. Available: 10.1016/j.ceramint.2019.05.308.

[15] A. Ekber Irmak, A. Coskun, E. Tasarkuyu, S. Akturk, G. Unlu, Y. Samancioglu, C. Sarikurkcu, B. Kaynar; A. Yucel, "The influence of the sintering temperature on the structural and the magnetic properties of doped manganites: $La_{0.95}Ag_{0.05}MnO_3$ and $La_{0.75}Ag_{0.25}MnO_3$", *Journal of Magnetism and Magnetic Materials*, vol. 322, no. 8, pp. 945-951, 2010. Available: 10.1016/j.jmmm.2009.11.029.